POLITECNICO DI TORINO
Repository ISTITUZIONALE

Modelling size effects for static strength of brittle materials

Original
Modelling size effects for static strength of brittle materials / Pagnoncelli, A. P.; Tridello, A.; Paolino, D. S.. - In: MATERIALS & DESIGN. - ISSN 0264-1275. - 195:(2020), pp. 1-12. [10.1016/j.matdes.2020.109052]

Availability:
This version is available at: 11583/2864672 since: 2021-01-21T13:57:52Z

Publisher:
Elsevier

Published
DOI:10.1016/j.matdes.2020.109052

Terms of use:

This article is made available under terms and conditions as specified in the corresponding bibliographic description in the repository

Publisher copyright

(Article begins on next page)

12 October 2024

Materials and Design 195 (2020) 109052

Contents lists available at ScienceDirect

Materials and Design

journal homepage: www.elsevier.com/locate/matdes

Modelling size effects for static strength of brittle materials

A.P. Pagnoncelli *, A. Tridello, D.S. Paolino

Department of Mechanical and Aerospace Engineering, Politecnico di Torino, Turin 10129, Italy

HIGHLIGHTS

- New size effect model for fracture strength of brittle materials
- Estimation of fracture strength considering specimen volume variation
- Statistical model based on the Largest Extreme Value Distribution
- Validation through uniaxial static tests data of brittle materials from literature

GRAPHICAL ABSTRACT

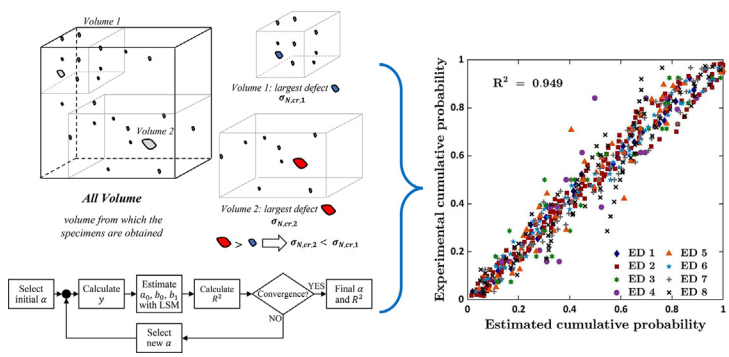

ARTICLE INFO

Article history:
Received 2 July 2020
Received in revised form 30 July 2020
Accepted 7 August 2020
Available online 11 August 2020

Keywords:
Size effects
Scaling
Uniaxial strength
Gumbel distribution
Defect size

ABSTRACT

The paper proposes a new model for the assessment of size effects affecting the fracture strength of brittle materials. The proposed model permits to accurately estimate the relation between the specimen strength, the initial defect size and to take into account the strength variation with respect to the tested volume.
The proposed methodology is analytically defined and thereafter validated with the literature data obtained through tests on different types of brittle materials, and on specimens with increasing volume. A simple procedure for parameter estimation is also defined in the paper. The literature validation proves the effectiveness of the proposed methodology, with the resulting fitting models in well agreement with the experimental dataset and characterized by high values of coefficients of correlation, similar or larger than those obtained in the literature with different approaches.

© 2020 The Author(s). Published by Elsevier Ltd. This is an open access article under the CC BY license (http://creativecommons.org/licenses/by/4.0/).

1. Introduction

In the last years, the use of advanced materials with brittle or quasi-brittle behavior, such as graphite, lightweight metallic alloys and high performance ceramics, has rapidly increased in many industrial application and sectors (automotive, machinery, electronic, aerospace, medical engineering). In order to safely employ these innovative materials, the research on the experimental assessment of their mechanical properties has gained a significant attention among researchers and universities. It is well-known in the literature that the experimental assessment of the mechanical properties of brittle materials and the modelling of their failure behavior are particularly difficult [1–6]. Indeed, the quasi-static behavior of brittle materials is governed by the population of defects, or better, by the distribution of the defect size within the material volume [1–4,7–9] and by the interaction between defects and microstructure. Moreover, the defect size is statistically dependent on the material volume [5,8–10], since the probability of large defects increases with the material volume (size or scale-effect), thus affecting the quasi-static properties. Due to its influence, size effects must be accurately modeled to properly assess the failure behavior of brittle materials. Mechanical

* Corresponding author.
E-mail addresses: ana.pagnoncelli@polito.it (A.P. Pagnoncelli), andrea.tridello@polito.it (A. Tridello), davide.paolino@polito.it (D.S. Paolino).

https://doi.org/10.1016/j.matdes.2020.109052
0264-1275/© 2020 The Author(s). Published by Elsevier Ltd. This is an open access article under the CC BY license (http://creativecommons.org/licenses/by/4.0/).

Nomenclature

a_0	initial crack size
a_{FPZ}	reference crack
$\sqrt{A_{global}}$	largest defect size contained in a specimen of volume $v_{tot.}$
f_t	tensile strength
$F_{S_{global}}(s_{MAX})$	global probability of rupture
n	degree of the polynomial equation
$P[S_{global} \geq s_{MAX}]$	reliability
p	probability of rupture
p_{est}	estimated probability of rupture
$\overline{p_{est}}$	mean estimated probability of rupture
p_{exp}	experimental probability of rupture
R^2	determination coefficient
v_{ref}	reference volume
v_{tot}	total volume of specimen
α	empirical coefficient of the proposed model
$\mu_{\sqrt{A}}$	Gumbel distribution parameter of location
$\mu_{\sqrt{A_{global}}}$	Gumbel distribution parameter of location relating to global largest defect size
S_{global}	global strength of the material
s_{MAX}	maximum applied stress
$\sigma_{\sqrt{A}}$	Gumbel distribution parameter of scale
$\sigma_{\sqrt{A_{global}}}$	Gumbel distribution parameter of scale relating to global largest defect size
σ_N	normal stress
$\sigma_{N,\,cr}$	stress at the critical point of the structure
$\sigma_{N,\,i}$	i-th maximum normal experimental stress

properties are generally estimated through tests on small specimens, but components are characterized by significantly larger stressed volumes. In order to prevent and avoid unexpected failures in large components, it has become crucial for researchers and industries to define design methodologies capable to reliably predict and model the mechanical strength of brittle material starting from laboratory tests. This would extend the range of application of materials with brittle behaviors, which is in many cases still limited due to the difficulty in modelling their failure behavior.

From an experimental point of view, the best solution to deal with size effects would be obviously to perform tests on full-scale components, but this is rarely possible and, generally, only very few full-scale components can be tested. If only few experimental tests are performed, it is hardly possible to properly assess the scatter associated to the mechanical strength due to the random distribution of defect size. Therefore, the critical defect size in the component volume should be predicted in almost all the cases by considering laboratory tests on small specimens. By considering the tensile strength, several models were proposed in the literature and validated experimentally [2–8] by testing specimens with increasing volumes. According to the models proposed in the literature, the main challenges for modelling size effects are two: i) to properly account for the large scatter of experimental results for the same specimen size; ii) to properly account for the volume effect on material strength, i.e. the tensile strength, and to define a model that is valid for different materials with brittle behaviors. The former challenge is mainly related to the random distribution of defect size. However, this issue can be relatively easily managed by increasing the number of valid test results for each specimen size, even if this could increase the testing and cost and in many cases the number of available specimens is limited.

The latter challenge is the most difficult one and, due to this, different methodologies have already been proposed in the literature. For example, Bažant, in [1], used the energy release rate associated to a crack present within the material to explain and describe specimen size effects on the fracture strength. In particular, based on the Size Effect Law (SEL) proposed in [1], several authors, in more recent years, have developed and discussed new models by proposing different initial equations for fracture energy. Some examples are the Boundary Effect Model (BEM), by Hu and Duan [2], the Size-Shape Effect Law from Hoover and Bažant [7] and the model proposed by Gao et al., in [3], which is a combination of both SEL and BEM. Other authors considered the use of Stress Intensity Factors to describe specimen's size effects on fracture strength, like in Karihaloo et al. [4]. All these models highlight the dependency between the mechanical strength and the initial critical defect size and its fundamental role on the failure process.

On the other hand, the inverse correlation between the specimen volume and the fracture strength of brittle materials is widely known in fracture mechanics. Since Weibull [10] proposed his probability distribution to describe the brittle materials fracture behavior, many authors [5,9,11–16] have applied it to materials with both brittle and quasi-brittle characteristics.

However, Danzer et al. [6] discussed, in their work, the validity of Weibull's statistics to evaluate specimen's size effects on fracture strength, concluding that it is only applicable under special conditions related to flaw distribution, flaw density and R-curve behavior.

Later on, Le et al. [9] proposed a model based on a compromise between energetic scaling and statistical scaling (i.e. SEL and Weibull statistics), stating that mechanical strength of specimens with strong stress singularities – for example, large flaws relative to structure size – can be more properly modeled with the energetic scaling model. On the contrary, specimens with very large volumes or no stress singularities follow the statistical scaling model. Therefore, the authors suggested a compromise between these two approaches through a generalized weakest-link model so as to predict fracture behavior of structures with intermediate stress singularities.

Lei, in [5], compared two statistical formulations based on Weibull statistics with the aim of finding a so called “master curve”, i.e., a curve that fits the fracture strength behavior of geometrically self-similar specimens of same material subdivided in sets of different volumes and submitted to the same loading condition. In particular, the experimental data coming from uniaxial tests on six types of materials obtained in literature were fitted by taking into account specimen volume effect and considering an exponential and a power function. All the methods proposed in the literature permit to accurately model size effects for brittle materials, but the best fit of the experimental data for each case is dependent on the material, on the loading condition and on the test type. On the other hand, a general methodology valid for a wide range of materials and loading conditions and that does not depend on the testing parameters is not currently available in the literature, to the authors' best knowledge.

In this paper, a new statistical model for assessing size effects on the static strength of brittle materials is proposed. Differently from the methodologies already proposed in the literature and based on the Weibull statistics [5,9,11–16], in the present model the influence of the specimen volume is accounted by considering the Gumbel distribution [17], a Largest Extreme Value Distribution (LEVD). Indeed, defects are randomly distributed within the specimen volume. The defect originating failure is the largest within the tested volume and the most critical. Therefore, the distribution of critical defect size is modeled by considering the largest defect in each specimen. According to [18], there is no correlation between defects (i.e., the defects are randomly distributed within the volume) and the probability of large defects increases with the volume (this is the rationale for size effects). Therefore, the LEVD permits to accurately account for the increment of the probability of critical defects within the tested volume, without implying a correlation between defects.

In the first part, the analytical formulation is provided and the procedure for parameter estimation is described. Thereafter, the model is validated on experimental data available in the literature, obtained by testing different types of materials (wood, concrete, coal seam, titanium

aluminide alloy, graphite and aluminum foam) and by performing tensile or compressive tests, confirming its effectiveness and general validity.

2. Model and methods

In this Section, the proposed methodology is described. In Section 2.1, the analytical formulation is provided. In Section 2.2, the procedure for parameters estimation is described.

2.1. Analytical formulation

As highlighted in the Introduction Section, the quasi-static strength of brittle materials is governed by the defect population within the material volume subjected to the largest applied stress. The mechanical strength of brittle materials should therefore be expressed as a function of the defect size. In the literature [1–3,7–9], the dependency between the maximum applied stress and the initial crack or defect size is generally assessed through energetic scaling models, based on different definitions for the fracture energy. Due to the first law of thermodynamics, the potential energy release rate must be equal to the energy consumed during cracking [1]. Therefore, according to the Hu-Duan Boundary Effect Model [2], $\sigma_{N,\ cr}$, the stress at the critical point (i.e. the defect resulting in the highest local stress), is given by:

$$\sigma_{N,cr} = \frac{f_t}{\sqrt{1+\frac{a_0}{a_{FPZ}}}} \propto \frac{1}{\sqrt{a_0}} \tag{1}$$

where, f_t is the tensile strength, a_0 is the initial crack or defect size and a_{FPZ} is the reference crack, proportional to the fully developed Fracture Process Zone (FPZ) in the large structure and determined by the intersection of strength and toughness criteria [2]. More generally, Eq. (1) points out that the mechanical strength is inversely proportional to the initial defect size a_0, according to the experimental evidence. In particular, the larger the defect, the smaller the quasi-static strength. However, not all defects present within the volume are critical: indeed, the final fracture originates from the largest defect. The distribution of the largest defects within the material volume therefore controls the quasi-static strength of brittle materials. Defects are randomly distributed within the material volume and large defects are statistically unlikely in small volumes (Volume 1 in Fig. 1). On the other hand, the probability of larger and more detrimental defects statistically increases with the material volume (Volume 2 in Fig. 1). Therefore, according to Eq. (1) and to Fig. 1, parts with large volumes show a smaller strength since critical defects are statistically larger.

According to Eq. (1) and Fig. 1, the strength of materials showing brittle behavior should be a function of defect size and loaded volume. By assuming a material body having a total stressed volume v_{tot} (e.g., the volume subjected to the largest stress amplitude in a mechanical test) with the largest defect of size $\sqrt{A_{global}}$, the global strength S_{global} can be defined in a general form:

$$\mathcal{S}_{global} = \left(\frac{f\left(\ln\left(\frac{v_{tot}}{v_{ref}}\right)\right)}{\sqrt{A_{global}}}\right)^{\alpha} \propto \frac{1}{\sqrt{A_{global}}^{\alpha}} \tag{2}$$

where $f\left(\ln\left(\frac{v_{tot}}{v_{ref}}\right)\right)$ is a function of the ratio $\frac{v_{tot}}{v_{ref}}$, being v_{ref} a reference volume, and α a constant parameter depending on the material. The dependency between the global strength and the volume was modeled by considering the logarithm of the ratio $\frac{v_{tot}}{v_{ref}}$, according to the Extreme Value Statistics. Indeed, the Largest Extreme Value distribution (LEVD) will be also used to account for the size effects associated to the defect size. Generally, for tests carried out on specimens with different volumes, v_{ref} corresponds to the smallest tested volume; it is worth to note that for $\frac{v_{tot}}{v_{ref}} = 1$, Eq. (2) provides the global strength for v_{ref}. The function $f\left(\ln\left(\frac{v_{tot}}{v_{ref}}\right)\right)$, since it depends on the ratio $\frac{v_{tot}}{v_{ref}}$, permits to account for size effects and can be expressed in the most simple form as a polynomial function with degree n. Accordingly, Eq. (2) can be rewritten as:

$$\mathcal{S}_{global} = \left(\frac{\sum_{j=0}^{n}\gamma_j\left(\ln\left(\frac{v_{tot}}{v_{ref}}\right)\right)^j}{\sqrt{A_{global}}}\right)^{\alpha} \tag{3}$$

being γ_j constant parameters that must be estimated from the experimental data and $j = 0, \ldots, n$. To summarize, according to Eq. (3), the global strength of the part depends on its volume – accounted by the polynomial equation of degree n – and on the largest defect size, $\sqrt{A_{global}}$. It is worth to note that that the larger the degree n, the larger is the capability of the model of modelling size effects and adapting to the experimental data. On the contrary, by increasing the degree n, the model becomes more complex and, even if the procedure for the parameter estimation is relatively easy (Section 2.2), it can increase the computational cost of the estimation. As a general rule, the degree n should be the smallest possible. For example, as will be shown and discussed in Section 3, a degree equal to 1 is enough to properly model size effects for a wide range of materials and testing conditions. Then, if the global strength of the part is larger than the maximum applied stress, the part will not fail. The reliability of the part is therefore the probability of having a global strength S_{global} larger than the maximum applied principal stress s_{MAX} in the component, as shown in Eq. (4):

$$P\left[\mathcal{S}_{global} \geq \int_{MAX}\right] = P\left[\left(\frac{\sum_{j=0}^{n}\gamma_j\left(\ln\left(\frac{v_{tot}}{v_{ref}}\right)\right)^j}{\sqrt{A_{global}}}\right)^{\alpha} \geq \int_{MAX}\right] \tag{4}$$

and, by substituting Eq. (3) in Eq. (4) and with easy passages, the reliability of the part becomes:

$$P\left[\mathcal{S}_{global} \geq \int_{MAX}\right] = P\left[\sqrt{A_{global}} \leq \frac{\sum_{j=0}^{n}\gamma_j\left(\ln\left(\frac{v_{tot}}{v_{ref}}\right)\right)^j}{\int_{MAX}^{1/\alpha}}\right] \tag{5}$$

The reliability of a part subjected to an applied stress equal to s_{MAX} can be also defined as a function of the probability of failure, $F_{S_{global}}(s_{MAX})$:

$$\mathrm{P}\left[\mathcal{S}_{\mathrm{global}} \geq \int_{\mathrm{MAX}}\right] = 1 - \mathrm{P}\left[\mathcal{S}_{\mathrm{global}} \leq \int_{\mathrm{MAX}}\right] = 1 - \mathrm{F}_{\mathcal{S}_{\mathrm{global}}}\left(\int_{\mathrm{MAX}}\right) \tag{6}$$

By substituting Eq. (5) in Eq. (6), the probability of failure, $F_{S_{global}}(s_{MAX})$ for a stress equal to s_{MAX} can be expressed as:

$$F_{\mathcal{S}_{global}}\left(\int_{MAX}\right) = 1 - P\left[\sqrt{A_{global}} \leq \sum_{j=0}^{n}\gamma_j\left(\ln\left(\frac{v_{tot}}{v_{ref}}\right)\right)^j \int_{MAX}^{-1/\alpha}\right] \tag{7}$$

According to Eq. (7), $F_{S_{global}}(s_{MAX})$ can be also expressed by considering the cumulative distribution function of $\sqrt{A_{global}}$, $F_{\sqrt{A_{global}}}$:

$$F_{\mathcal{S}_{global}}\left(\int_{MAX}\right) = 1 - F_{\sqrt{A_{global}}}\left(\sum_{j=0}^{n}\gamma_j\left(\ln\left(\frac{v_{tot}}{v_{ref}}\right)\right)^j \int_{MAX}^{-1/\alpha}\right) \tag{8}$$

Eq. (8), which was analytically derived by modifying the physical model for failure of brittle materials reported in Eq. (1), shows that the probability of failure of a part with volume v_{tot} and subjected to maximum stress equal to s_{MAX} depends on the distribution of defect size within the part or, more correctly, on the distribution of the largest defects within the part volume.

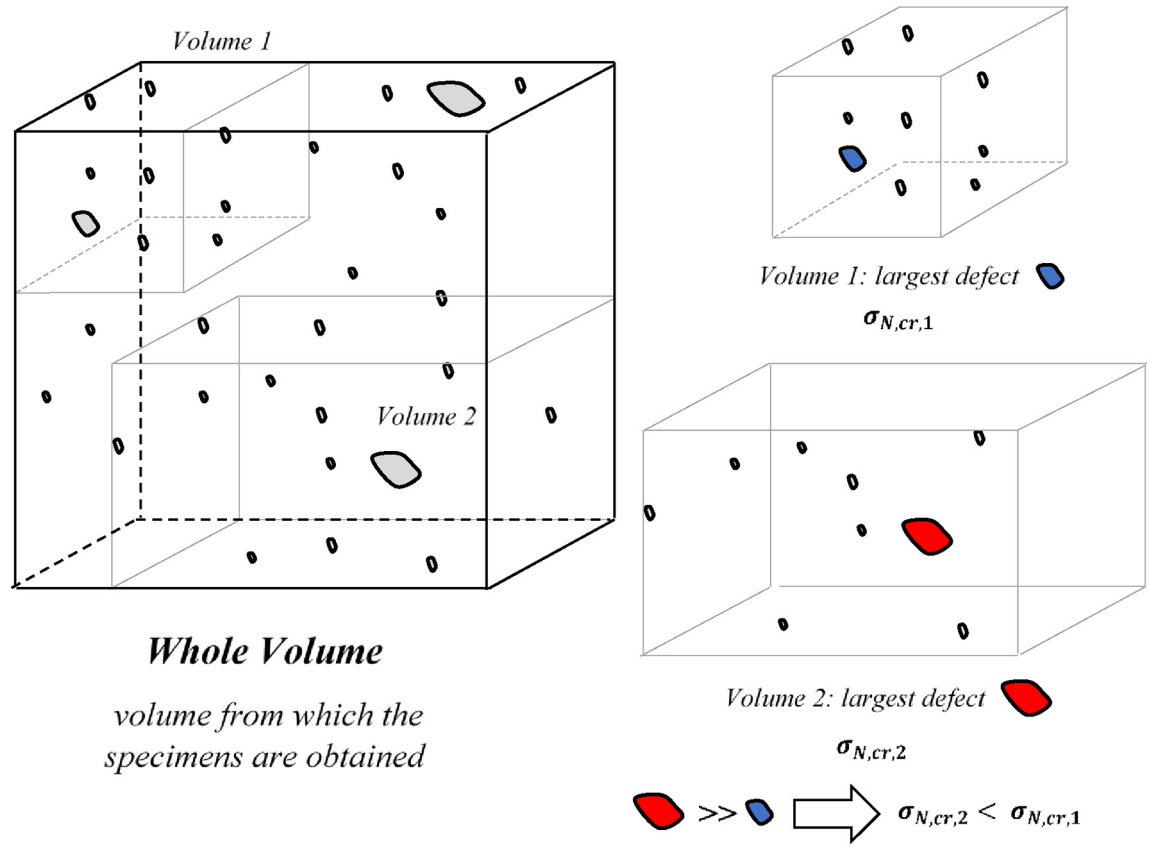

Fig. 1. Schematic representation of size effects: statistical increment of the critical defect with the material volume.

The distribution of the largest defects within the material volume should therefore be considered for properly assessing the probability of failure of brittle materials. According to the literature [19–23], in the present model $F_{\sqrt{A_{global}}}$ is assumed to follow a Gumbel LEVD with parameters $\mu_{\sqrt{A_{global}}}$ and $\sigma_{\sqrt{A_{global}}}$ that depend on the ratio $\frac{v_{tot}}{v_{ref}}$:

$$F_{\sqrt{A_{global}}}\left(\sqrt{a_{global}}\right) = e^{-e^{-\frac{\sqrt{a_{global}}-\mu_{\sqrt{A_{global}}}}{\sigma_{\sqrt{A_{global}}}}}} \tag{9}$$

with $\mu_{\sqrt{A_{global}}} = \mu_{\sqrt{A}} + \sigma_{\sqrt{A}} \cdot \ln\left(\frac{v_{tot}}{v_{ref}}\right)$ and $\sigma_{\sqrt{A_{global}}} = \sigma_{\sqrt{A}}$, being $\mu_{\sqrt{A}}$, $\sigma_{\sqrt{A}}$ constant parameters. By substituting Eq. (8) in Eq. (9), the probability of failure $F_{S_{global}}(s_{MAX})$ can be finally expressed as:

$$F_{S_{global}}(\int_{MAX}) = 1-e^{-e^{-\frac{\sum_{j=0}^{n}\gamma_j\left(\ln\left(\frac{v_{tot}}{v_{ref}}\right)\right)^j \int_{MAX}^{-1/\alpha} - \left(\mu_{\sqrt{A}}+\sigma_{\sqrt{A}}\cdot\ln\left(\frac{v_{tot}}{v_{ref}}\right)\right)}{\sigma_{\sqrt{A}}}}} \tag{10}$$

Eq. (10) provides a general formulation for the probability of failure of a part with volume v_{tot} and subjected to an applied stress equal to s_{MAX}. It depends on the ratio $\frac{v_{tot}}{v_{ref}}$ and therefore permits to account for size effects. The constant parameters $\alpha, \mu_{\sqrt{A}}, \sigma_{\sqrt{A}}$ and γ_j have to be estimated from the experimental data according to the procedure shown in the following Section. Once the constant parameters were estimated from experimental tests on specimens with small volumes, Eq. (10) permits to assess the i-th quantile of the fracture strength for the component volume and can therefore be employed for the component design.

2.2. Parameter estimation

According to Eq. (10), the constant parameters $\alpha, \mu_{\sqrt{A}}, \sigma_{\sqrt{A}}$ and γ_j are to be estimated from the results of experimental tests. By substituting $x = \ln\left(\frac{v_{tot}}{v_{ref}}\right)$ and $y = s_{MAX}^{-1/\alpha}$ and through easy passages, Eq. (10) can be rewritten as follows:

$$F_{S_{global}}(\int_{MAX}) = 1-e^{-e^{-\sum_{j=0}^{n}\frac{\gamma_j}{\sigma_{\sqrt{A}}}x^j y + \frac{\mu_{\sqrt{A}}}{\sigma_{\sqrt{A}}} + x}} \tag{11}$$

The double exponential distribution in Eq. (11) can be linearized by computing the logarithm of the first and the second member, two times:

$$\ln\left(-\ \ln\left(1-F_{S_{global}}(\int_{MAX})\right)\right) = \frac{\mu_{\sqrt{A}}}{\sigma_{\sqrt{A}}} + x - \sum_{j=0}^{n}\frac{\gamma_j}{\sigma_{\sqrt{A}}}x^j y \tag{12}$$

By substituting $a_0 = \frac{\mu_{\sqrt{A}}}{\sigma_{\sqrt{A}}}$ and $b_j = \frac{\gamma_j}{\sigma_{\sqrt{A}}}$, Eq. (12) can be rewritten as follows:

$$\ln\left(-\ \ln\left(1-F_{S_{global}}(\int_{MAX})\right)\right) = a_0 + x + b_0 y + \sum_{j=1}^{n} b_j x^j y \tag{13}$$

Eq. (13) can be finally rewritten by introducing the variable $z^* = \ln\left(-\ln\left(1-F_{S_{global}}(s_{MAX})\right)\right) - x$, and by expressing z^* as a function of the independent variable y and of the constant unknown coefficients a_0, b_0 and b_j:

$$z^* = a_0 + b_0 y + \sum_{j=1}^{n} b_j x^j y \tag{14}$$

For the simplest case of specimens subjected to a uniform stress distribution throughout the volume (e.g., tensile or compressive tests, with a uniform stress distribution within the gage length), the degree n of the polynomial equation in Eq. (3) is the lowest one, equal to 1. Accordingly, the system of equations that has to be solved is reported in Eq. (15):

$$z^* = a_0 + b_0 y + b_1 xy, \text{ where } \begin{cases} z^* = \ln(-\ln(1-p)) - \ln\left(\frac{v_{tot}}{v_{ref}}\right) \\ x = \ln\left(\frac{v_{tot}}{v_{ref}}\right) \\ y = \int_{MAX}^{-1/\alpha} \\ a_0 = \frac{\mu_{\sqrt{A}}}{\sigma_{\sqrt{A}}} \\ b_0 = -\frac{\gamma_0}{\sigma_{\sqrt{A}}} \\ b_1 = -\frac{\gamma_1}{\sigma_{\sqrt{A}}} \end{cases} \tag{15}$$

being $p = F_{S_{global}}(s_{MAX})$. The system in Eq. (15) can be solved to estimate the unknown constant parameters a_0, b_0 and b_1, from which the parameters $\mu_{\sqrt{A}}$, $\sigma_{\sqrt{A}}$, γ_0 and γ_1 involved in the model in Eq. (10) can be finally obtained.

Fig. 2 shows the flow-chart of the iterative procedure developed to estimate the coefficients α, a_0, b_0 and b_1 from the experimental data. The procedure was implemented in the Matlab software.

According to Fig. 2, firstly a tentative value of the parameter α is randomly chosen in a predetermined interval (in this case [−1000 : 1000]), which should have a range wide enough to enable an exhaustive optimization of α, but should also avoid extensive computation time. Given α, the y value can be obtained according to Eq. (15) by considering the maximum applied stress, s_{MAX}. It is worth to note that, for each experimental failure due to a maximum stress equal to s_{MAX}, a corresponding value of y must be defined. Thereafter, the coefficients a_0, b_0 and b_1 can be estimated from Eq. (14) through the application of the Least Squares Method (LSM):

$$\boldsymbol{\beta} = (\boldsymbol{M}'\boldsymbol{M})^{-1}\boldsymbol{M}'(\boldsymbol{z}^* - \boldsymbol{x}), \text{ where } \boldsymbol{M} = [\boldsymbol{1}\ \ \boldsymbol{y}\ \ \boldsymbol{xy}] \text{ and } \boldsymbol{\beta} = \begin{Bmatrix} a_0 \\ b_0 \\ b_1 \end{Bmatrix} \tag{16}$$

where $\boldsymbol{\beta}$ is the vector of the unknown parameters that have to be estimated, whereas $\boldsymbol{M}$ is the design matrix. $\boldsymbol{M}$ has a number of rows equal to the number of experimental data. For each experimental failure which occurred in a specimen with volume v_{tot} and subjected to a maximum stress equal to s_{MAX}, the z^* value is computed by considering the corresponding experimental probability of failure p. In particular, for the i-th specimen, p was estimated with the Benard's approximation for Median Ranks [23]:

$$p\left(\sigma_N \le \sigma_{N,i}\right) = \frac{i - 0.3}{N + 0.4} \tag{17}$$

where N is the total number of specimens for each volume group. This method was chosen because it permits to accurately approximate the median rank, according to [24] and is generally used in models for the assessment of size effects for brittle materials [5]. Other methods for the estimation of p could also be employed, but with limited and negligible influences on the estimated parameters.

Finally, the coefficient of determination R^2 is computed according to Eq. (18):

$$R^2 = 1 - \frac{\sum\left(p_{exp} - p_{est}\right)^2}{\sum\left(p_{exp} - \overline{p_{exp}}\right)^2} \tag{18}$$

being p_{exp} the experimental cumulative probability as calculated in Eq. (17) and p_{est} the cumulative probability estimated according to Eq. (10) and with $\mu_{\sqrt{A}}$, $\sigma_{\sqrt{A}}$, γ_0 and γ_1 values obtained from α, a_0, b_0 and b_1. The α value is iteratively varied with the objective of maximizing the R^2 value.

According to the procedure shown in this Section, even if many parameters are involved in the model, the procedure for parameters estimation is quite simple. Only one parameter is optimized, whereas the other parameters are obtained through a simple application of the Least Squares Method. An optimization algorithm based on the Simplex method was implemented in the Matlab software. Different starting values for α are considered for the experimental validation of the model in Section 3 to verify a possible dependency between α and the initial tentative value. However, for a large range of search – such as [−1000 : 1000], which corresponds to the interval selected for all the simulations conducted in this work – the model converges to the optimized solution in limited time, always smaller than 1 s, and it has found to be independent on the starting α, thus proving the effectiveness of the proposed procedure.

3. Results and discussion

In this Section the proposed methodology is validated on experimental datasets taken from the literature. In particular, in Section 3.1, the experimental data available in the literature is considered for the validation. In Section 3.2, the potentialities of the proposed methodology are discussed, and its fitting capability is compared to the other methodologies available in the literature.

3.1. Experimental validation

The experimental data are obtained from tables where possible [11,12,25,26], and by using the software Engauge Digitizer to extract data points from graphs if the tables are not available [13–15,27].

The coefficient of determination of the fitting models available in Lei [5] is considered for the sake of comparison. In particular, in Lei [5], the coefficient of determination was assessed on the so called "master

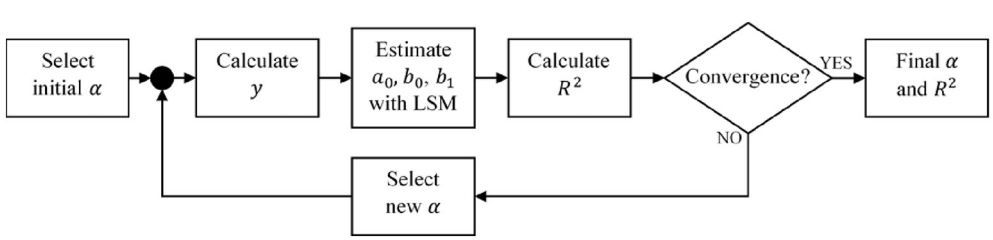

Fig. 2. Flow chart of the procedure developed for the parameter estimation.

curves" which plot a "compound parameter", correlated to the failure probability, with respect to the considered mechanical strength. The experimental data on the master curves were interpolated by considering an exponential function and a power function as material functions. Since the compound parameter depends on the cumulative probability, the coefficient of determination R^2 obtained through the exponential and the power fitting is considered for the sake of comparison.

3.1.1. Tensile strength of wood

The first dataset that is considered for the validation of the proposed methodology is taken from [13]. In particular, [13] reports experimental data on the tensile strength of the soft-wood *Picea abies*, which is widely used for load bearing timber structures in Europe. Two sets of specimens with different sizes were manufactured in order to assess the volume effect on the tensile strength parallel to fiber direction. All specimens were cut from one single log and selected to be free of knots and other visible defects. Fig. 3a shows a schematic image of the specimens used by the authors [13], along with an indication of the wood fibers direction.

Fig. 3b shows the data obtained by Dill-Langer et al. [13] for the two sets of specimens. In particular, the abscissa axis reports the tensile strength, whereas the ordinate axis shows the cumulative probability. The markers in the figure are the experimental cumulative probability, computed according to Eq. (16), whereas the curves represent the fitting based on Eq. (10). According to Eq. (10), a reference volume, v_{ref}, of 420 mm3, corresponding to the volume of the smallest specimens, is considered for the parameter estimation. The degree of the polynomial function was chosen equal to 1. The volumes considered in Fig. 3b are calculated from the dimensions of the cross-section and of the gauge length for each set of specimens, according to [13].

According to Fig. 3, the proposed model permits to well fit the experimental data in [13]. The coefficient of determination R^2, estimated according to Eq. (18), is equal to $R^2 = 0.986$, which is slightly larger to the values obtained in Lei [5], being equal to $R^2 = 0.975$ with the power fitting model and $R^2 = 0.960$ with the exponential fitting model.

In Moshtaghin et al. [25], size effects on the tensile strength parallel to fiber orientation of Norway spruce wood was analyzed. The configuration of the test, the geometry of the specimens and the wood fiber direction were the same as those in [13], as shown in Fig. 4a. Differently from Fig. 3, a larger number of volumes was tested. In particular, the tested specimens were divided in four groups, each with a different gauge length (ranging from 2 mm to 128 mm) and with the same cross-sections.

In Fig. 4b, the cumulative probability with respect to the tensile strength is reported. In particular, the experimental data in [25] together with the estimated models are shown in the figure. The reference volume is set equal to 8 mm3, corresponding to the smallest tested volume in [25]. The degree of the polynomial function was chosen equal to 1. The volumes shown in Fig. 4b are calculated with the cross-section and gauge length reported in [25].

The proposed model is in well agreement with the experimental data also for this type of wood. The model, in particular, fits well the experimental data for the small volumes, whereas the fitting is slightly worse for the largest volume (512 mm^3), whose experimental data presents a different behavior when compared to the other volumes. The smallest volume (8 mm^3) also shows a slight discrepancy towards its fitting curve since the experimental data for the three smallest volumes (8 mm^3, 32 mm^3 and 128 mm^3) are somewhat overlapped. As the estimation procedure optimizes the parameters that maximize the fitting and the experimental data shows this unexpected distribution, the accuracy of the general estimation is not as good as for the other cases discussed in this work. Nevertheless, the coefficient of determination R^2 is close to 1, being equal to 0.974. In Lei [5], R^2 was equal to 0.974 with the power fitting model and to $R^2 = 0.962$ with the exponential fitting. The proposed model has therefore the same fitting capability of the power law fitting model proposed in Lei [5].

Finally, the model was validated on the results obtained by Pedersen et al. [11] by testing a Norwegian grown spruce (*Picea abies*). In this case, the tensile strength perpendicular to the fiber direction was assessed, as represented in Fig. 5a, containing an indication of the wood fibers direction in the specimens. According to Pedersen et al. [11], the specimens were carefully selected from a large population of boards and did not contain knots and other macroscopic defects. The specimens, of equal cross-sections, were divided into four groups with increasing gauge lengths, from 25 mm to 230 mm, following the geometry of Fig. 5a. The volumes indicated in Fig. 5b were calculated by using the measures for the cross-section and specimen lengths presented in [11]. In this case, a $v_{ref} = 8.4 \cdot 10^4$ mm³, corresponding to the smallest

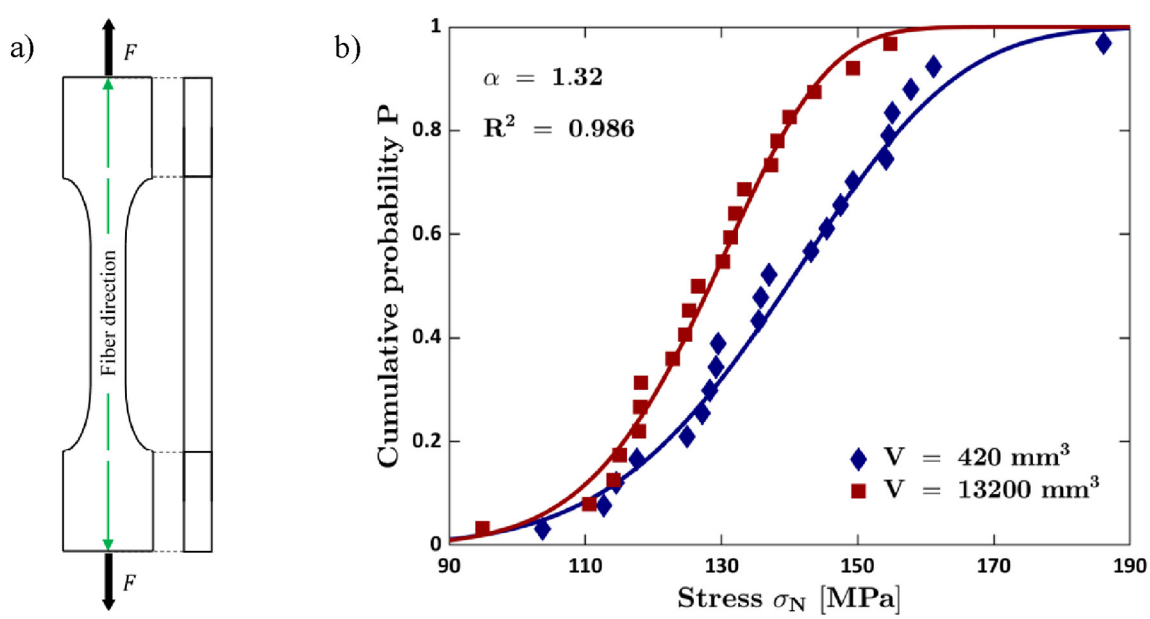

Fig. 3. Soft-wood of the species spruce (*Picea abies*) [13]: (a) schematic image of the specimens; (b) Cumulative probability with respect to the longitudinal tensile strength of a soft spruce wood: experimental data and fitting curve.

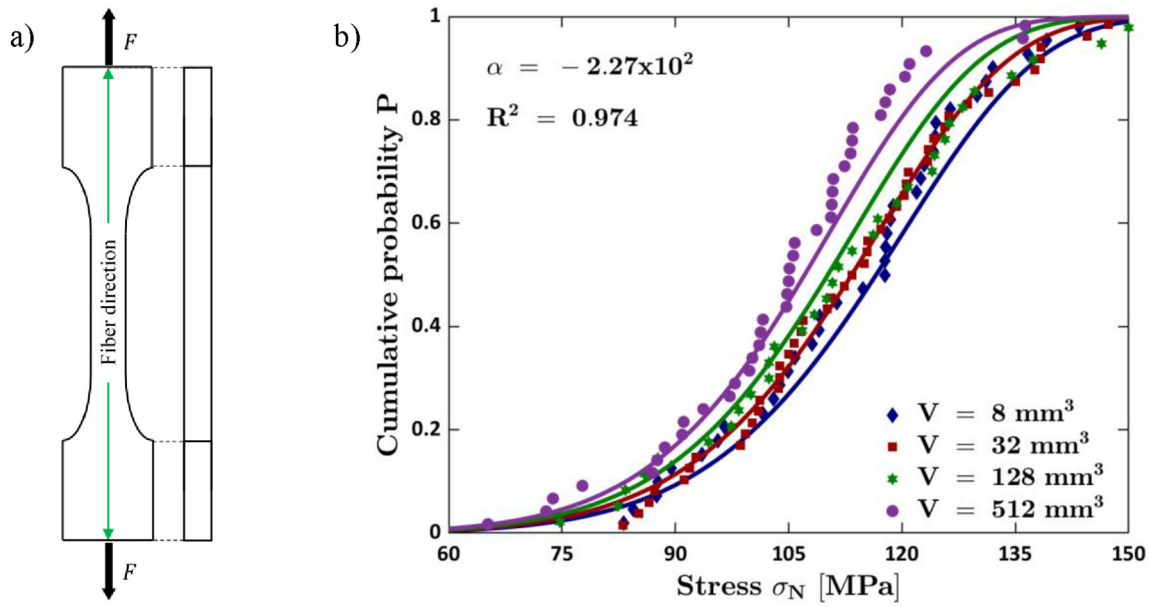

Fig. 4. Norway spruce wood [25]: (a) schematic representation of the tested specimens; (b) cumulative probability with respect to the longitudinal tensile strength of a Norway spruce wood: experimental data and fitting curve.

tested volume, is considered. The degree of the polynomial function was chosen equal to 1. Fig. 5b shows the cumulative probability with respect to the transversal tensile strength: the experimental data and the fitting curves are reported.

According to Fig. 5b, the model is in well agreement with the experimental data. The coefficient of determination R^2 is equal to 0.918, slightly smaller than the R^2 in Figs. 3b and 4b, mainly due to the smaller number of experimental data. On the other hand, in Lei [5], R^2 was found to be equal to 0.918 with the power fitting model and to 0.846 with the exponential fitting. As for Fig. 5b, the proposed model has thus the same capability of modelling size effects as the power fitting model reported in [5].

According to the results reported in this Section, the proposed formulation proved effective in modelling size effects of wood, by considering both the longitudinal strength (Figs. 3b and 4b) and the transversal strength (Fig. 5b). The fitting models are in well agreement with the experimental data, with R^2 valued larger or at least equal than the values obtained in the literature.

3.1.2. Double-punch tests of concrete cylinders

The proposed methodology is validated by considering the tensile strength of concrete in Marti [26]. In particular, in Marti [26], double-punch test on ready-mix concrete cylinders were carried out to assess size effects. According to Marti [26], the volume of the tested cylinders can be calculated as $V = \pi d^3/4$, being d the specimen's diameter. Each of the five sets of specimens, with the geometry schematically shown in Fig. 6a had a different diameter. A reference volume of $3.4 \cdot 10^5$ mm³, corresponding to the smallest tested volume, is considered. The degree of the polynomial function was chosen equal to 1. Fig. 6b

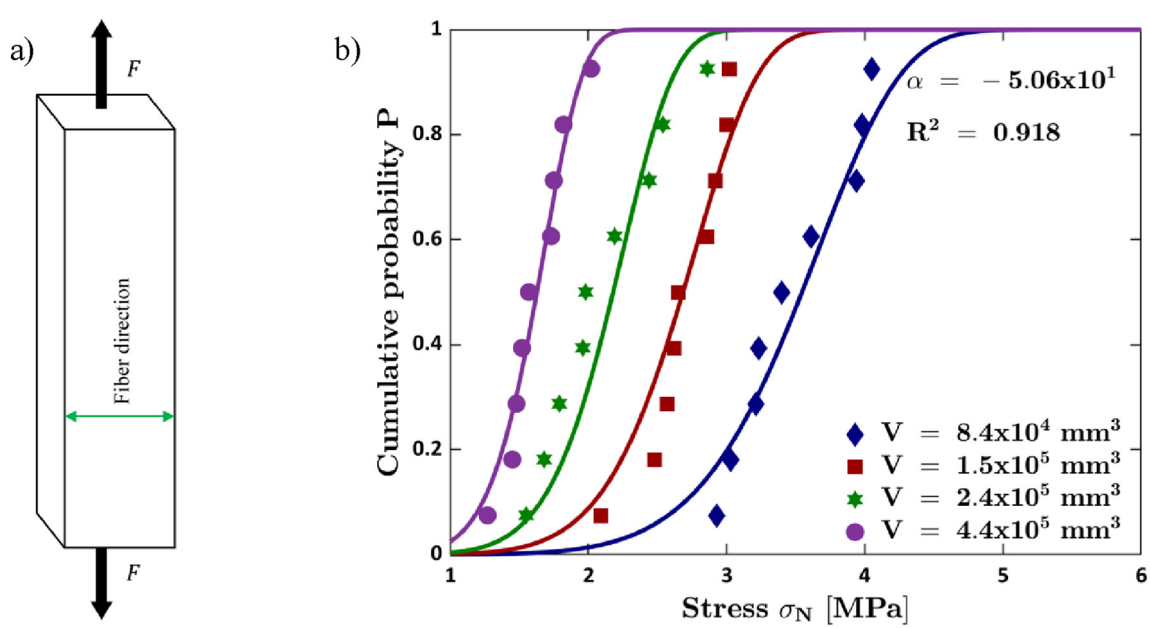

Fig. 5. Norwegian grown spruce (*Picea abies*) [11]: (a) schematic representation of the tested specimens; (b) Cumulative probability with respect to the tensile strength perpendicular to the fiber direction: experimental data and fitting curve.

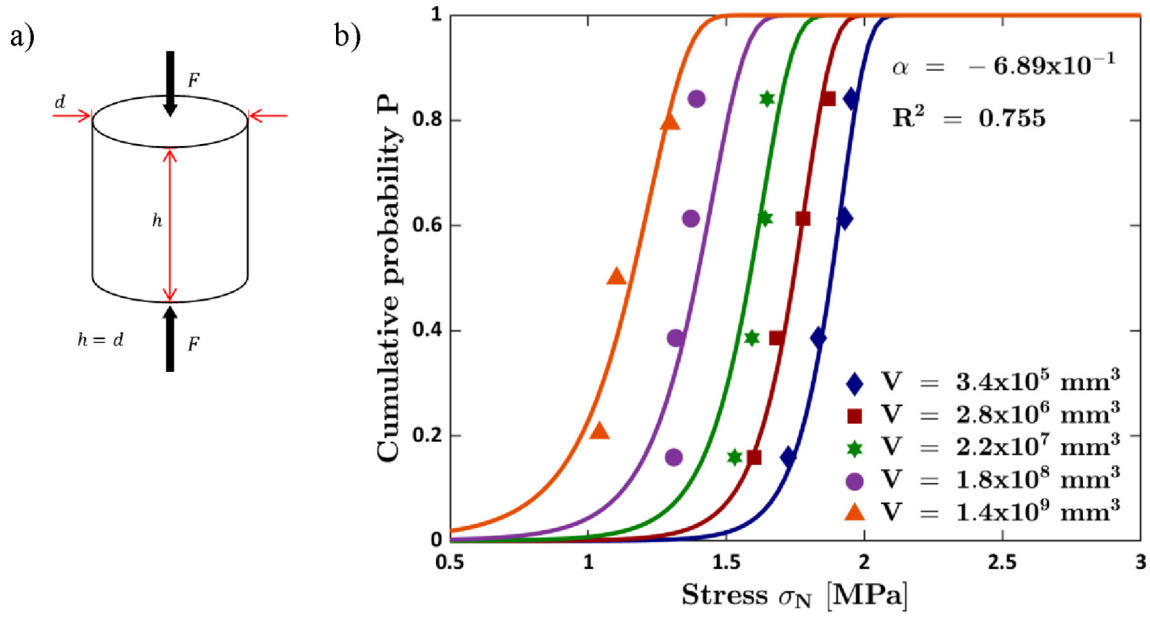

Fig. 6. Double-punch test on ready-mix concrete cylinders [26]: (a) Schematic of the tested specimens; (b) Cumulative probability with respect to the compression strength of concrete cylinders: experimental data and fitting curve.

shows the cumulative probability with respect to the tensile strength: the experimental data and the fitting curves are reported.

According to Fig. 6b, the R^2 value is equal to 0.755, which is lower than those obtained for wood, but in this case a smaller number of experimental data is available (i.e., 3 test results for each volume compared to at least 9 for wood). However, the R^2 values obtained with the proposed formulation are larger than those obtained in Lei [5], being equal to 0.547 for the power fitting model and to $R^2 = 0.670$ for the exponential fitting model.

3.1.3. Uniaxial compression tests of coal seam

In Gonzatti et al. [27], a large number of experimental data on the compression strength of coal seam was experimentally obtained. The coal seam was extracted and then cut and finished with diamond saws to produce the specimens. In particular, 56 uniaxial compression tests were carried out on six sets of cubic specimens with increasing volumes. Fig. 7a depicts the tested specimen geometries, whose volumes is $V = \ell^3$, being ℓ the measure of the side of the cube for each set of specimens, as reported in [27]. A reference volume of $1.7 \cdot 10^5$ mm³, corresponding to the smallest tested volume, is considered. The degree of the polynomial function was chosen equal to 1. Fig. 7b shows the cumulative probability with respect to the compression strength: the experimental data and the fitting curves are reported.

According to Fig. 7, the R^2 value for the proposed model is equal to 0.924. It is worth to note that model is in well agreement with the experimental data for volumes up to 8.1 10^6 mm^3, whereas for larger volumes the fitting is worse, but a limited number of experimental data is available (e.g., for the largest tested volume of $3.1 \cdot 10^7$ mm3 only two data are present as well as for 1.6 10^7 mm^3, the second largest volume). The R^2 values for the power fitting model and for the exponential fitting

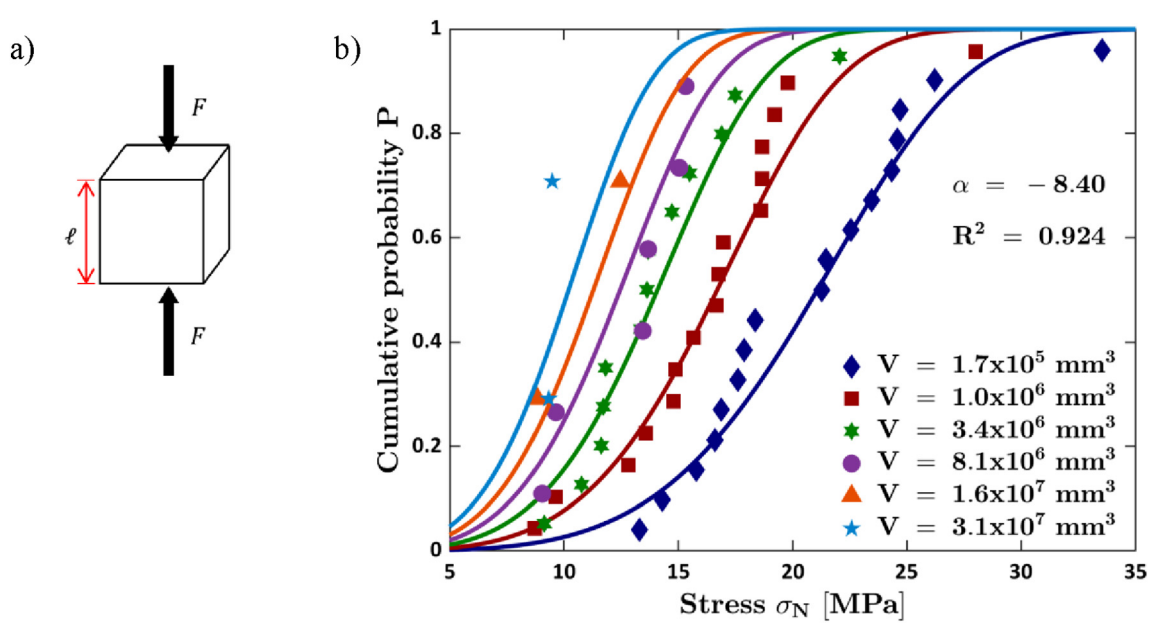

Fig. 7. Compression strength of coal seam [27]: (a) schematic representation of the tested specimens (b) cumulative probability with respect to the compression strength of coal seam: experimental data and fitting curve.

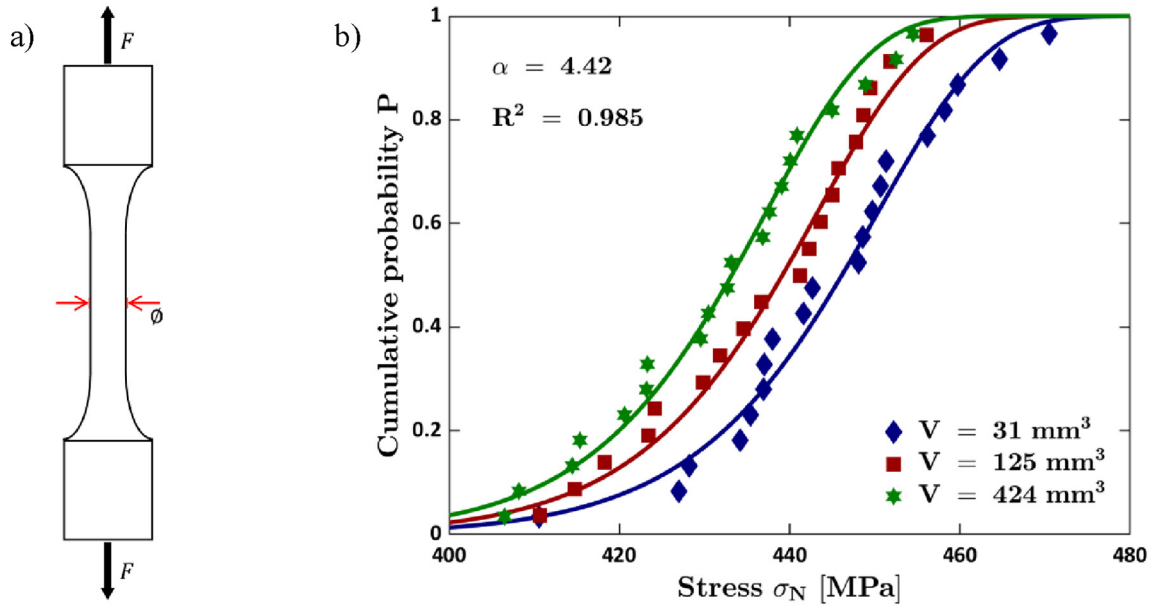

Fig. 8. Tensile strength of gamma titanium aluminide alloy, Ti-48Al-2Cr-2Nb [14]: (a) schematic representation of the tested specimens; (b) Cumulative probability with respect to the tensile strength of a Ti-48Al-2Cr-2Nb alloy: experimental data and fitting curve.

in Lei [5], are equal to 0.922 and to 0.884, respectively. The proposed formulation has therefore the same fitting capability of the power fitting model in Lei [5].

3.1.4. Uniaxial tensile tests of gamma titanium aluminide alloy

In Dresbach et al. [14], the tensile strength of gamma titanium aluminide alloy, Ti-48Al-2Cr-2Nb, used for manufacturing the turbine blades of aircraft engines, was experimentally assessed. Three groups of cylindrical specimens, characterized by different diameters ∅ and gauge lengths, were tested in [14] and are schematically shown in Fig. 8a. A reference volume of 31 mm³, corresponding to the smallest tested volume, is considered. The degree of the polynomial function was chosen equal to 1. Fig. 8b shows the cumulative probability with respect to the compression strength: the experimental data and the fitting curves are reported. The volumes reported in the legend of Fig. 8b are the same as in [14].

According to Fig. 8b, also in this case the coefficient of determination is in agreement with literature results. In particular, in the proposed model it is equal to 0.985, the same value obtained in Lei [5], with the power fitting and slightly larger than the R^2 value obtained with the exponential fitting (0.984).

3.1.5. Uniaxial tensile tests of nuclear grade graphite

Size effects on the tensile strength of an NBG-18 Nuclear Grade Graphite was experimentally assessed in Yoon et al. [15]. Four cylindrical specimen groups, each with different diameters and gauge

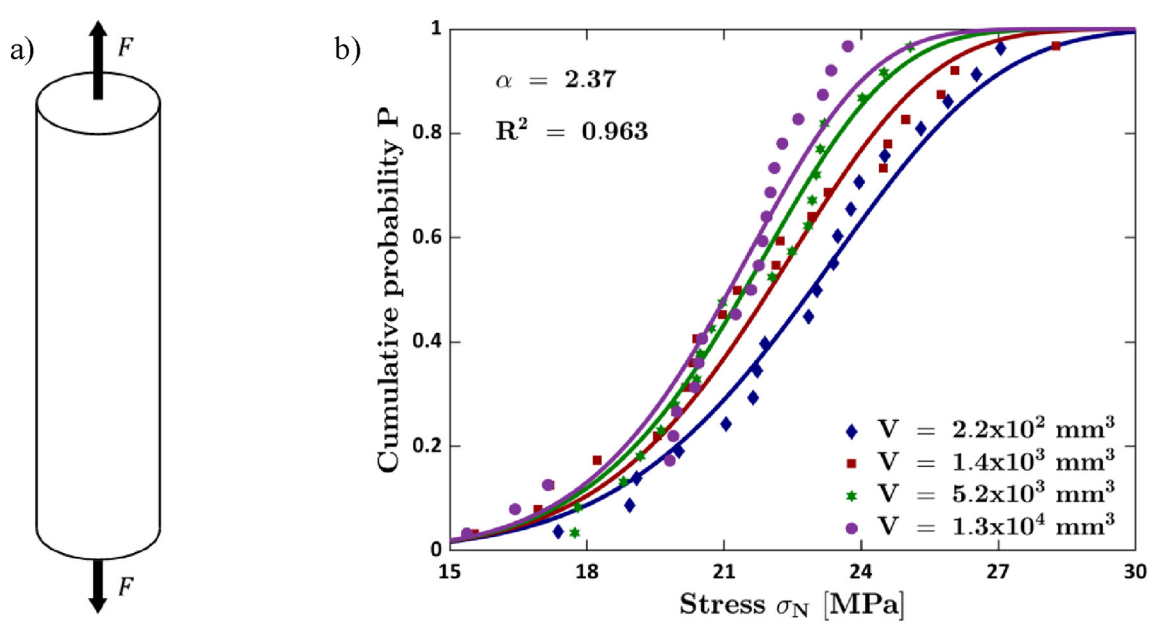

Fig. 9. Tensile strength of a NBG-18 nuclear grade graphite [15]: (a) Schematic of the tested specimens (b) Cumulative probability with respect to the tensile strength of a NBG-18 nuclear grade graphite: experimental data and fitting curve.

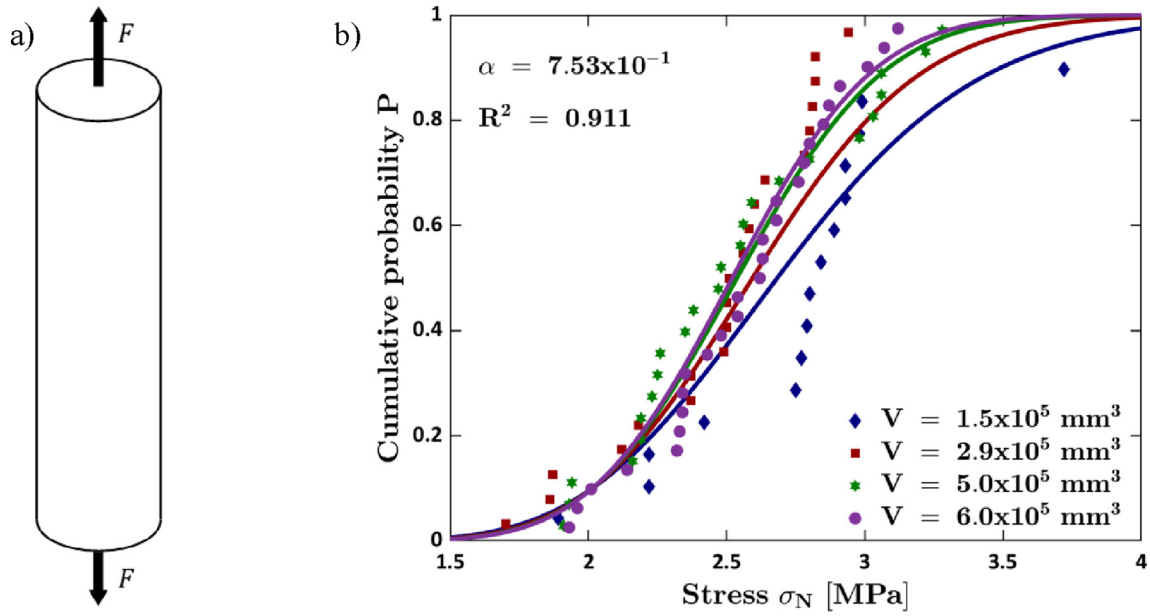

Fig. 10. Tensile strength of an Aluminum Foam [12]: (a) schematic representation of the tested specimens; (b) Cumulative probability with respect to the tensile strength of an Aluminum Foam: experimental data and fitting curve.

lengths, were tested in Yoon et al. [15]: the specimen geometry is schematically shown in Fig. 9a. A reference volume of $2.2 \cdot 10^2$ mm³, corresponding to the smallest tested volume, is considered. The degree of the polynomial function was chosen equal to 1. Fig. 9b shows the cumulative probability with respect to the tensile strength: the experimental data and the fitting curves are reported. The volumes reported in Fig. 9b are calculated from the diameter and length of the specimens used in [15].

Also for the Nuclear Grade Graphite, the R^2 value is larger than 0.90 (0.963) and close to the values obtained in Lei [5] with the power fitting method ($R^2 = 0.960$) and the exponential fitting ($R^2 = 0.963$).

3.1.6. Uniaxial tensile tests of aluminum foam

Finally, the proposed methodology is validated on the tensile strength of Aluminum Foam, characterized by a brittle behavior. In Blazy et al. [12], tensile tests on cylindrical specimens fabricated from flat plates of aluminum foam were carried out. Four groups of cylindrical specimens with increasing gauge length and diameter were tested in order to assess the volume effect on the tensile strength. The specimen geometry is schematically shown in Fig. 10a. A reference volume of $1.5 \cdot 10^5$ mm³, corresponding to the smallest tested volume, is considered. The degree of the polynomial function was chosen equal to 1. Fig. 10b also shows the cumulative probability with respect to the tensile strength: the experimental data and the fitting curves are shown. The volume for each specimen group is calculated from the diameter and length reported in [12].

Table 1
Values for the parameters obtained for each set of experimental data.

Dataset	R^2	α	a_0	b_0	b_1
ED 1	0.986	1.32	$1.01 \cdot 10^1$	$-4.40 \cdot 10^2$	$-3.16 \cdot 10^1$
ED 2	0.974	$-2.27 \cdot 10^2$	$-1.72 \cdot 10^3$	$1.68 \cdot 10^3$	$-8.28 \cdot 10^{-1}$
ED 3	0.918	$-5.06 \cdot 10^1$	$-3.49 \cdot 10^2$	$3.40 \cdot 10^2$	2.21
ED 4	0.756	$-6.91 \cdot 10^{-1}$	$-1.38 \cdot 10^1$	5.42	$-1.53 \cdot 10^{-1}$
ED 5	0.924	−8.40	$-3.85 \cdot 10^1$	$2.65 \cdot 10^1$	$-2.99 \cdot 10^{-1}$
ED 6	0.985	4.42	$1.58 \cdot 10^2$	$-6.28 \cdot 10^2$	−2.35
ED 7	0.963	2.37	$1.85 \cdot 10^1$	$-7.07 \cdot 10^1$	−3.03
ED 8	0.911	$7.53 \cdot 10^{-1}$	3.70	$-1.51 \cdot 10^1$	−2.53

Fig. 10b shows that, for the smallest volume, the experimental data has a visible deviation from its fitting curve. This fact can be explained by the irregular distribution of the data collected for this volume associated with its reduced number of samples (16 specimens) when compared to the other three volumes with, respectively, from the smallest to the largest volume, 21, 24 and 27 specimens. The estimation optimizes the parameters to maximize the fitting capability to all the available data, therefore reducing the accuracy for the volumes with smaller numbers of samples or the cases where the results diverge considerably from the general behavior. Nevertheless, also for the Aluminum Foam, the model is in good agreement with the experimental data, with a coefficient of determination of 0.911. According to Lei [5], the R^2 values are smaller, being equal to 0.900 for the power fitting and to 0.877 for the exponential fitting.

3.2. Discussion

According to Section 3.1, the methodology proposed in Section 2 proved to be effective in assessing size effects of materials that experimentally show a brittle behavior. In particular, the methodology was validated on materials with completely different characteristics, such as wood, coal seam, Nuclear Grade Graphite and metallic materials (Ti-48Al-2Cr-2Nb and Aluminum Foam). For all materials, the coefficient of determination was found to be larger than 0.90, apart from concrete cylinders ($R^2 = 0.76$), but in this case the reason was the small amount of specimen tested (4 or less for each volume set). Moreover, the model was validated also by analyzing size effects on different mechanical properties (longitudinal tensile strength, transversal tensile strength, compressive strength) and for different type of tests (tensile test, compressive test, double-punch tests) and, in all the cases, it provided high values of R^2. Accordingly, the experimental validation confirmed that the general formulation defined in Section 2 is capable of accurately modelling size effects on different mechanical properties and for different testing types.

The procedure for parameter estimation described in Section 2.2 proved also to be effective. Indeed, the optimization of the α parameter permits to accurately adapt the model to the material tested and the procedure was easy and time-efficient:

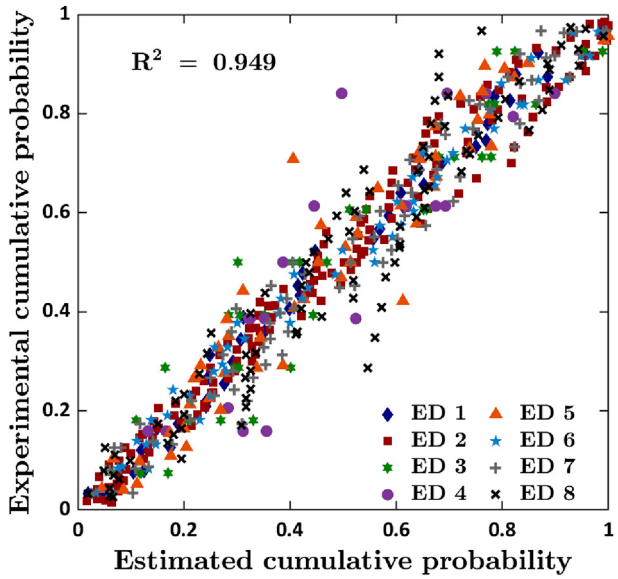

Fig. 11. Probability-Probability (P–P) plot of the experimental literature data considered for the validation of the proposed model.

in all the cases, the optimization process took less than 1 s. The model, moreover, permits to deal with size effects both for small volume range, like as for Norway spruce wood (from 8 mm³ to 512 mm³) and for very large volume range, like as for concrete cylinders (from 10^5 mm³ to 10^9 mm³). The choice of the smallest tested volume as the reference volume v_{ref} was verified to be effective in all the tested cases.

The degree of the polynomial function for modelling the strength in Eq. (3) has been chosen equal to 1 in all the cases, proving that, also with the simplest formulation, the proposed model is capable of properly dealing with size effects for a wide range of materials and testing conditions. However, the degree of the polynomial function can be increased if different specimen geometries and loading conditions are considered, to properly adapt to the experimental data. In general, $n = 1$ should be at first considered and then increased if the model does not properly fit with the experimental data.

Furthermore, according to experimental validation, the proposed model has different fitting accuracy for different material types and sizes. Nonetheless, the model is applicable to any brittle material at any volume range. However, it is possible that, when the size variation among the different sets of specimens is very large, the estimation might encompass a loss of accuracy, which can be recovered by increasing the degree of the polynomial equation n, in Eq. (3).

Table 1 shows the values of the parameters estimated according to the procedure described in Section 2.2. The numeration of the experimental data (ED) present in Table 1 is reported in the following:

- ED 1 – longitudinal tensile strength of soft spruce wood as in Fig. 3);
- ED 2 – longitudinal tensile strength of Norway spruce wood as in Fig. 4;
- ED 3 – transversal tensile strength of Norway spruce wood as in Fig. 5;
- ED 4 – double-punch tests of concrete cylinders as in Fig. 6;
- ED 5 – uniaxial compression tests of coal seam as in Fig. 7;
- ED 6 – uniaxial tensile tests of gamma titanium aluminide alloy as in Fig. 8;
- ED 7 – uniaxial tensile tests of Nuclear Grade Graphite as in Fig. 9;
- ED 8 – uniaxial tensile tests of Aluminum Foam as in Fig. 10.

In order to further validate the proposed methodology, all the experimental data considered in the present paper were reported in the Probability-Probability plot shown in Fig. 11. In particular, the experimental probability, calculated according to Eq. (16), is plotted with respect to the estimated cumulative probability, calculated according to Eq. (10). The numeration of the experimental data (ED) follows the same notation from Table 1.

According to Fig. 11, the markers coming from the different sets of literature experimental data are concentrated in the region of the bisector between the two axes, with an overall coefficient of determination of 0.949. The P–P plot further confirms that the proposed methodology is capable of efficiently modelling size effects for materials showing a brittle behavior.

Table 2 compares the R^2 values obtained in the present paper with those obtained in Lei [5] on the "master curves" by considering a "power fitting" and an "exponential fitting". For each material, the highest R^2 value is highlighted.

According to Table 2 and as highlighted in the previous Sections, the R^2 values obtained with the proposed methodology are equal or larger than the R^2 values obtained in the literature. In particular, they are larger in 4 out 8 cases and equal in the remaining 4. Moreover, depending on the material and on the experimental tests, either the exponential fitting or the power fitting provides larger R^2 values. On the other hand, the proposed formulation permits to obtain the best fitting without a priori choice of the fitting method, thus demonstrating its general validity.

Despite the proposed model exhibiting a fitting capability equal or larger than other methods available in the literature, it is not possible to assure that it is better than other models. Indeed, the theoretical base of the proposed formulation (use of the LEVD) is completely different from that of other models [5], where the Weibull statistics and the Weakest-Link Principle for the material resistance are considered. However, the validation with literature datasets has proved that the proposed model represents a valid alternative to other methodologies, with a high capacity to adapt to different materials and testing

Table 2
Summary of the experimental results: R^2 values obtained by fitting the data with the proposed model (Eq. (10)) and with the models in Lei [5].

		R^2		
	Mechanical properties	Present paper	Exponential fitting (Lei [5])	Power fitting (Lei [5])
Soft spruce wood	Tensile strength	0.986	0.960	0.975
Norway spruce wood	Tensile strength	0.974	0.962	0.974
Norway spruce wood	Transversal tensile strength	0.918	0.918	0.846
Concrete Cylinders	Tensile strength	0.755	0.670	0.547
Coal Seam	Compression strength	0.924	0.922	0.884
Ti-48Al-2Cr-2Nb	Tensile strength	0.985	0.984	0.985
NBG-18 nuclear grade graphite	Tensile strength	0.963	0.963	0.960
Aluminum Foam	Tensile strength	0.911	0.877	0.900

The underline serves to indicate the highest obtained value of R^2 for each material between the present paper, the exponential fitting (Lei) and the power fitting (Lei).

conditions and characterized by a reliable and relatively easy procedure for parameter estimation.

4. Conclusion

In the present paper an innovative generalized formulation for assessing size effects on the quasi-static mechanical properties of materials showing a brittle behavior was proposed.

The analytical formulation was at first defined. In particular, differently from the majority of literature models which are based on the Weibull distribution, the proposed formulation successfully applied the Gumbel Distribution to deal with size effects of brittle materials. The material strength as a function of the volume was accurately modeled and it was derived from a macro-mechanical model describing the crack initiation process in brittle materials.

A general procedure for parameter estimation was also defined. Despite its complexity, the constant coefficients can be estimated through a simple linear regression and only one parameter, α, depending on the material and on the testing condition, needs to be estimated with an optimization procedure. The procedure, implemented in the Matlab software, proved to be effective and time-efficient: in all the cases, the optimization process took less than 1 s.

Finally, the proposed formation was validated on experimental datasets available in the literature. Its generalized formulation was shown to properly model size effects for different materials showing brittle behavior (wood, coal seam, graphite, concrete, metallic materials and foam) and for different testing conditions (tensile test, compressive test, double punch tests). The coefficient of determination was found to be larger or at least equal to that found in the literature for the same tested material. Moreover, differently from literature models, the proposed formulation permits to obtain the best fitting without a priori choice of the fitting method for the experimental data, thus demonstrating its general validity.

To conclude, the proposed model proved to be general and effective in dealing with size effects of materials showing a brittle behavior and can be reliably used for the analysis of experimental results obtained by testing specimens with increasing loaded volumes or to estimate the strength of components characterized by large volumes.

Declaration of Competing Interest

None

References

[1] Z.P. Bažant, Size effect in blunt fracture: concrete, rock, metal, J. Eng. Mech. 110 (1984) 518–535.
[2] X. Hu, K. Duan, Size effect and quasi-brittle fracture: the role of FPZ, Int. J. Fract. 154 (2008) 3–14.
[3] X. Gao, G. Koval, C. Chazallon, Energetical formulation of size effect law for quasi-brittle fracture, Eng. Fract. Mech. 175 (2017) 279–292.
[4] B.L. Karihaloo, H.M. Abdalla, Q.Z. Xiao, Size effect in concrete beams, Eng. Fract. Mech. 70 (2003) 979–993.
[5] W.-S. Lei, A generalized weakest-link model for size effect on strength of quasi-brittle materials, J. Mater. Sci. 53 (2018) 1227–1245.
[6] R. Danzer, P. Supancic, J. Pascual, T. Lube, Fracture statistics of ceramics – Weibull statistics and deviations from Weibull statistics, Eng. Fract. Mech. 74 (2007) 2919–2932.
[7] C.G. Hoover, Z.P. Bažant, Comparison of the Hu-Duan boundary effect model with the size-shape effect law for quasi-brittle fracture based on new comprehensive fracture tests, J. Eng. Mech. 140 (2014) 480–486.
[8] X. Hu, J. Guan, Y. Wang, A. Keating, S. Yang, Comparison of boundary and size effect models based on new developments, Eng. Fract. Mech. 175 (2017) 146–167.
[9] J.-L. Le, M. Pieuchot, R. Ballarini, Effect of stress singularity magnitude on scaling of strength of quasi-brittle structures, J. Eng. Mech. 140 (2014).
[10] W. Weibull, A statistical theory of the strength of materials, Ingeniorsvetenskapakademiens Handlinger 151 (1939) 1–45.
[11] M.U. Pedersen, C.O. Clorius, L. Damkilde, P. Hoffmeyer, A simple size effect model for tension perpendicular to the grain, Wood Sci. Technol. 37 (2003) 125–140.
[12] J.-S. Blazy, A. Marie-Louise, S. Forest, Y. Chastel, A. Pineau, A. Awade, C. Grolleron, F. Moussy, Deformation and fracture of aluminium foams under proportional and non-proportional multi-axial loading: statistical analysis and size effect, Int. J. Mech. Sci. 46 (2004) 217–244.
[13] G. Dill-Langer, R.C. Hidalgo, F. Kun, Y. Moreno, S. Aicher, H.J. Herrmann, Size dependency of tension strength in natural fiber composites, Physica A 325 (2003) 547–560.
[14] C. Dresbach, T. Becker, S. Reh, J. Wischek, S. Zur, C. Buske, T. Schmidt, R. Tiefers, A stochastic reliability model for application in a multidisciplinary optimization of a low pressure turbine blade made of titanium aluminide, Latin American J. Solids Struct. 13 (2016) 2316–2332.
[15] J.H. Yoon, T.S. Byun, J.P. Strizak, L.L. Snead, Characterization of tensile strength and fracture toughness of nuclear graphite NBG-18 using subsize specimens, J. Nucl. Mater. 412 (2011) 315–320.
[16] W.-S. Lei, G. Qian, Z. Yu, F. Berto, Statistical size scaling of compressive strength of quasi-brittle materials incorporating specimen length-to-diameter ratio effect, Theor. Appl. Fract. Mech. 104 (2019) 102345.
[17] E. Gumbel, Statistics of Extremes, Columbia University Press, New York, 1958.
[18] W.A. Curtin, Tensile Strength of Fiber-Reinforced Composites: III. Beyond the Traditional Weibull Model for Fiber Strengths, J. Comp. Mater. 34 (2000) 1301–1332.
[19] Y. Murakami, Metal Fatigue: Effects of Small Defects and Nonmetallic Inclusions, 1st ed Elsevier Ltd, Oxford, 2002.
[20] K.V. Anderson, S.R. Daniewicz, Statistical analysis of the influence of defects on fatigue life using a Gumbel distribution, Int. J. Fatigue 112 (2018) 78–83.
[21] S. Beretta, Y. Murakami, Statistical analysis of defects for fatigue strength prediction and quality control of materials, Fatigue Fract. Eng. Mater. Struct. 21 (2002) 1049–1065.
[22] D.S. Paolino, A. Tridello, G. Chiandussi, M. Rossetto, S-N curves in the very-high-cycle fatigue regime: statistical modeling based on the hydrogen embrittlement consideration, Fatigue Fract. Eng. Mater. Struct. 39 (2016) 1319–1336.
[23] D.S. Paolino, A. Tridello, G. Chiandussi, M. Rossetto, Estimation of P-S-N curves in very-high-cycle fatigue: statistical procedure based on a general crack growth rate model, Fatigue Fract. Eng. Mater. Struct. 41 (2018) 718–726.
[24] A. Benard, E.C. Bos-Levenbach, The plotting of observations on probability paper, Statististica Neerlandica 7 (1953) 163–173.
[25] A.F. Moshtaghin, S. Franke, T. Keller, A.P. Vassilopoulos, Experimental characterization of longitudinal mechanical properties of clear timber: random spatial variability and size effects, Constr. Build. Mater. 120 (2016) 432–441.
[26] P. Marti, Size effect in double-punch tests on concrete cylinders, ACI Mater. J. 86 (1990) 597–601.
[27] C. Gonzatti, L. Zorzi, I.M. Agostini, J.A. Fiorentini, A.P. Viero, R.P. Philipp, In situ strength of coal bed based on the size effect study on the uniaxial compressive strength, Int. J. Min. Sci. Technol. 24 (2014) 747–754.